Advanced Materials '93, VI / Frontiers in
Materials Science and Engineering, edited by S. Sōmiya et al.
Trans. Mat. Res. Soc. Jpn., Volume 19B



# SOME FRONTIER R&D ASPECTS OF ADVANCED INORGANIC MATERIALS DEVELOPMENT

Dong-Sheng YAN

State Key Lab on High Performance Ceramics and Superfine Microstructure, Shanghai Institute of Ceramics, Chinese Academy of Sciences, Shanghai 200050, CHINA

Abstract: In this paper, the following frontier R&D areas for advanced inorganic materials are discussed. These include: (1) Enchancing the capability of materials design; (2) Processing, microstructure and properties of advanced ceramics; (3) Strengthening and toughening of advanced ceramics; and (4) Bioceramics and their superfine microstructure studies. The major intention of this overview is to attract comments and discussions with an aim to stimulate new ideas for the advancement of this important branch of materials science and engineering.

**Key Words:** Advanced Ceramics, Phase Relationship Studies, Materials Design, Microstructure and Properties, Strengthening and Toughening, Bioceramics, Superfine Microstructure

## INTRODUCTION

It is commonly envisaged that materials science and engineering is one of the few cornerstones for hi-tech development in the nineties and beyond. And advanced inorganic materials have been predicted to have an even faster pace of development in comparison with other major types of new materials in terms of market share and applications.

The frontier R&D problems for advanced inorganic materials are multifaceted. In this lecture, a few areas of research will be addressed, which to the author's judgement are among the important ones that the materials community should be on the alert to participate and watch their advancements. However, it is more so the intention to arouse discussion and assessment on the priority issues of research in advanced inorganic materials. Whereby, recommendations may be generated for the consideration and deliberation of the science policy makers and funding agencies, as well as to promote interdisciplinary and international collaboration.

## ENCHANCING THE CAPABILITY OF MATERIALS DESIGN

Speaking of materials design, there are different levels — atomic and electronic, molecular, microscopic, and macroscopic — that scientists are striving to design the materials to meet with the performance requirements more intelligently. This endeavor depends very much on the type of materials they are dealing with and the depth of understanding they can master at the moment. In many cases, advanced and sophisticated equipments are of no less importance. Therefore, there will be endless footprints that may be recognized as landmarks of advancements in materials design.

Advanced ceramics is a broad class of materials with a microstructure usually in the micron and submicron scale which is composed of major crystalline phase(s) and grain boundary phase(s). Both the crystalline phase(s) and the grain boundary phase(s) have their influence on the properties of the materials whether these be mechanical, electrical, ferroelectric, piezoelectric, or semiconductive, etc. In this paper, we will restrict our subject matter on advanced structural ceramics and in this passage, the design of silicon nitride materials with high performance mechanical properties will be addressed.

Advanced silicon nitride ceramics is a family of materials that has exhibited extremely

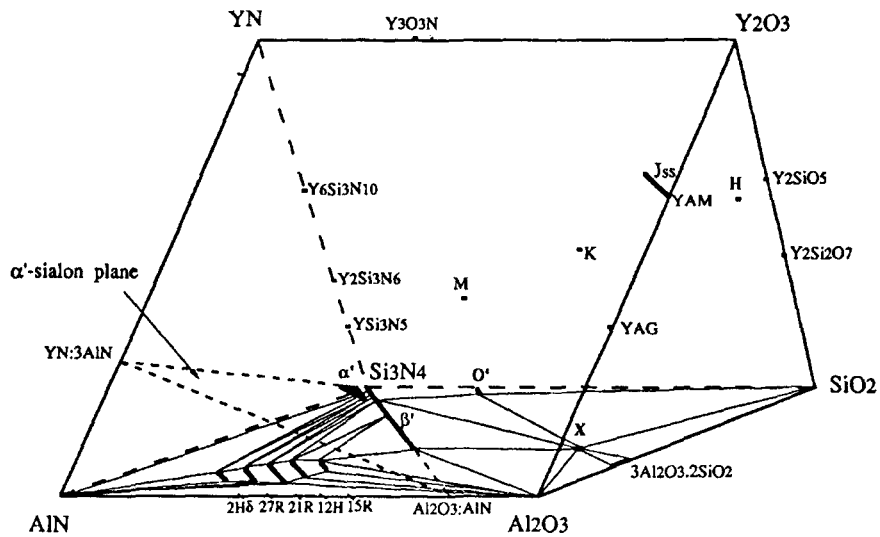


Fig.1 The sub-solidus phase relationships of Y,Si,Al/O, N system showing the solid solutions and AlN polytypoids

encouraging properties especially at high temperatures. However, oxide additives are necessary to achieve full densification through liquid phase diffusion and sintering. The possibility for compositional design of such complex systems has been a subject of intensive research in recent years. It is realized that a comprehensive knowledge of the phase equilibrium relationships between different constituents is essential. Complex M-Si-Al-O-N systems (M=Na, Li, Mg, Ca, Y, and rare earth elements) have been extensively studied in more recent years[14]. These research results show that there are several important solid solutions in those systems: β'-Sialon, α'-Sialon, O'-Sialon and AlN polytypoids (Fig. 1) and each has its own typical crystalline morphology and physical characteristics. A brief summary can be stated as follows: β'-Sialon, a solid solution of β-$Si_3N_4$ with a general formula of $Si_{6-z}Al_zO_zN_{8-z}$ where $O<Z<4.2$, possesses high fracture strength and toughness; α'-Sialon, a solid solution of α-$Si_3N_4$ represented as $M_xSi_{12-(m+n)}Al_{m+n}O_nN_{16-n}$, has higher hardness and better thermal shock resistance; O'Sialon, a solid solution of $Si_2N_2O$ with $Al_2O_3$, shows better oxidation resistance. AlN-polytypoids usually have an elongated platelet or even fibrous morphology, but their behavior in a microstructure has been much less studied and less known. Besides, there are a number of new compounds in these systems. The significance of phase relationship studies of silicon nitride systems is thus, to provide information for: (a) the search of effective sintering additives; (b) the design of nitride ceramics with desirable major phases; and (c) the tailoring of grain boundary phases.

We will take the Y-Si-Al-O-N system as a model to illustrate the approach for compositional design of advanced nitride ceramics. After around ten years' work in close collaboration with several world renowned laboratories, the phase relationship of this multi-component system has been fully delineated[13,14]. There are, altogether, 76 compatibility regions in this whole system and some of them are of particular interest as a guidance for the design of compositions that may show good performance especially at high temperatures. The following are a few promising combinations:

- β$Si_3N_4$ or β'-Sialon — Refractory Grain Boundary Phases
- α'-Sialon or α'-β'-Sialons — Refractory

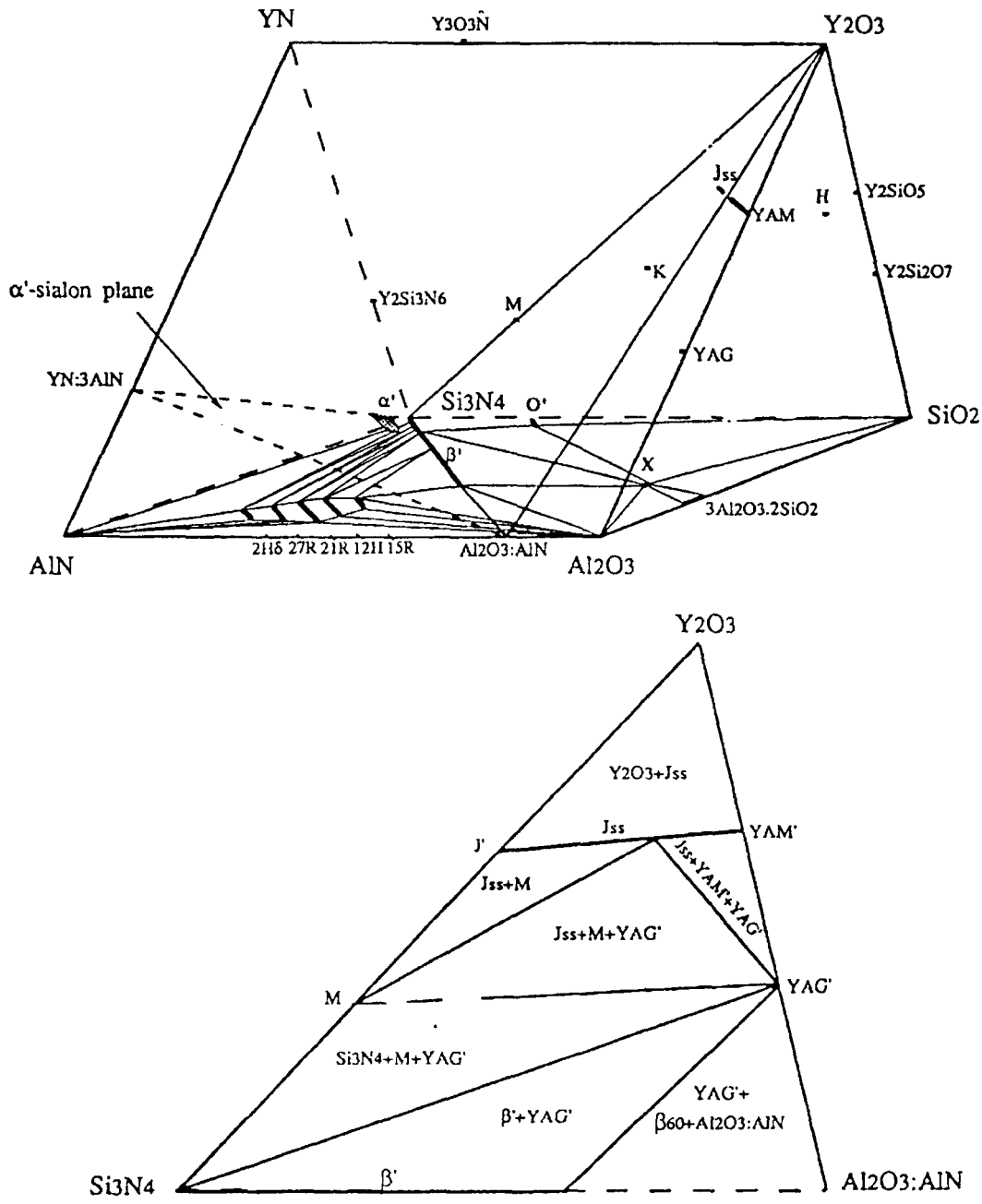


Fig. 2 Sub-solidus phase relationships in the $Si_3N_4$-$Y_2O_3$-$Al_2O_3$:AlN System[18]

Grain Boundary Phases

●α'-Sialon — AlN Polytypoids — Refractory Grain Boundary Phases

●β'-Sialon — AlN Polytypoids — Refractory Grain Boundary Phases

●O'-Sialon — β'-Sialon — Refractory Grain Boundary Phases

Some of the potential compatibility regions are shown in Fig. 2-5.

This approach for materials design has

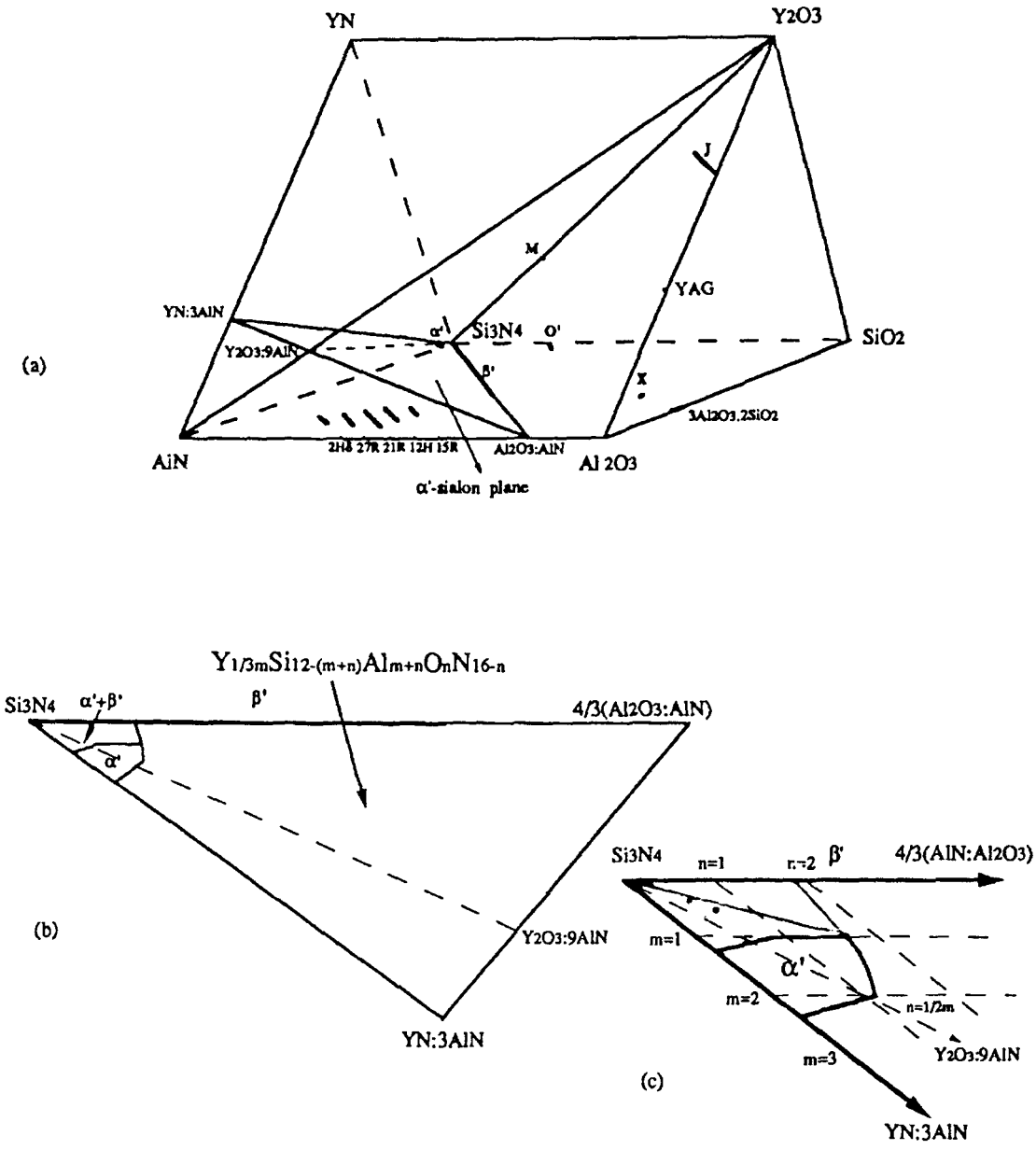


Fig. 3 Representation of α'-Sialon phase in Y-Si-Al-O-N system[31]

shown to be effective and some encouraging results have been obtained.

The following example shows an attempt to have $\beta$-$Si_3N_4$ or $\beta$'-Sialon as the major crystalline phase and try to upgrade the material property by manipulating the grain boundary phase.

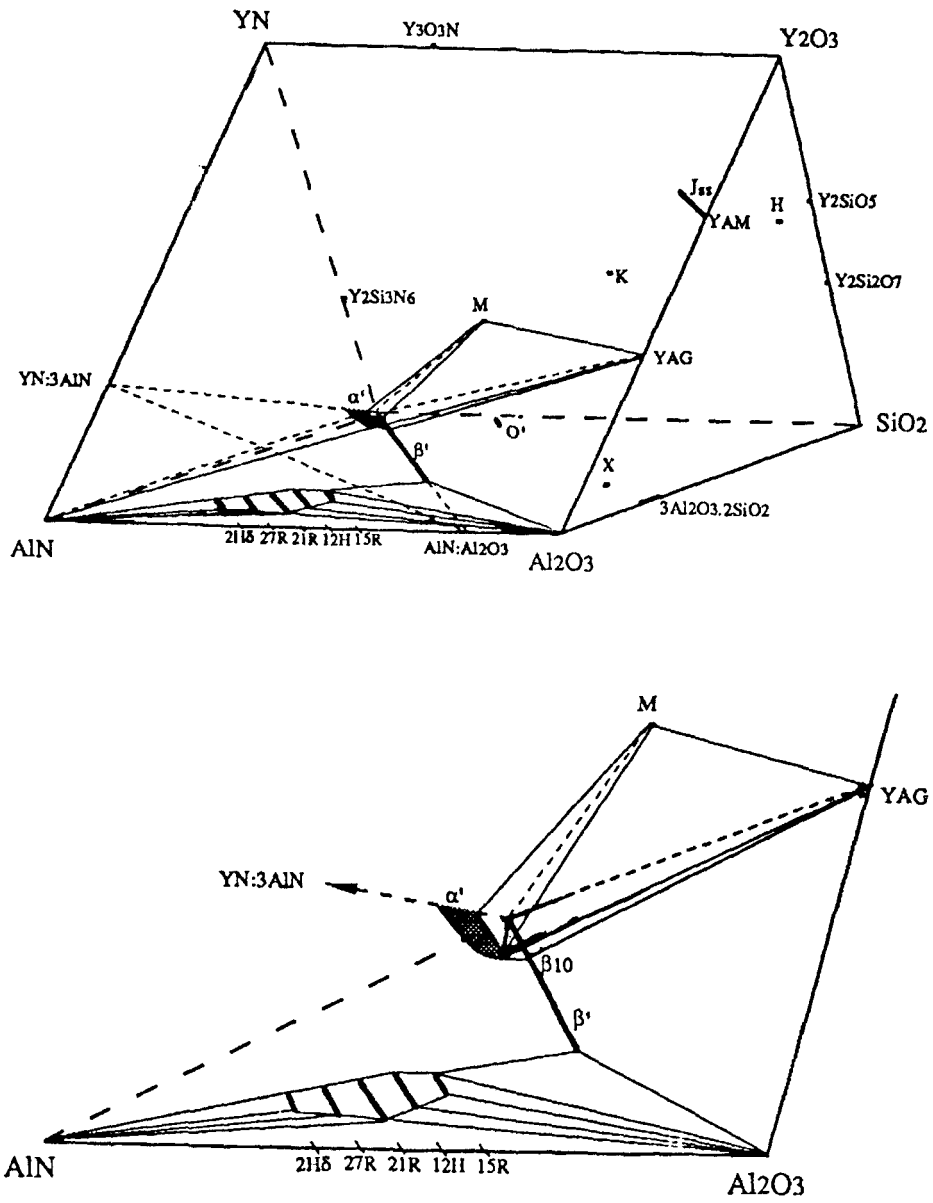


Fig. 4 α'-β' two phase region with melilite (M) and garnet (YAG) phases

$Y_2O_3$ and $Al_2O_3$ compound additives are now commonly used to fabricate $Si_3N_4$ ceramics with good properties. However, with the surface $SiO_2$ present along with silicon nitride powders as starting materials, the lowest eutectic temperature of $SiO_2$-$Al_2O_3$-$Y_2O_3$ system is not high. The attempt was to replace $Al_2O_3$ by a rare earth oxide by which the eutectic temperature of the system of oxide can be raised by about 200°C[15]. Under such circumstances, the glassy phase that remained at the grain boundaries after sintering will be much more refractory. Moreover, post-sintering heat

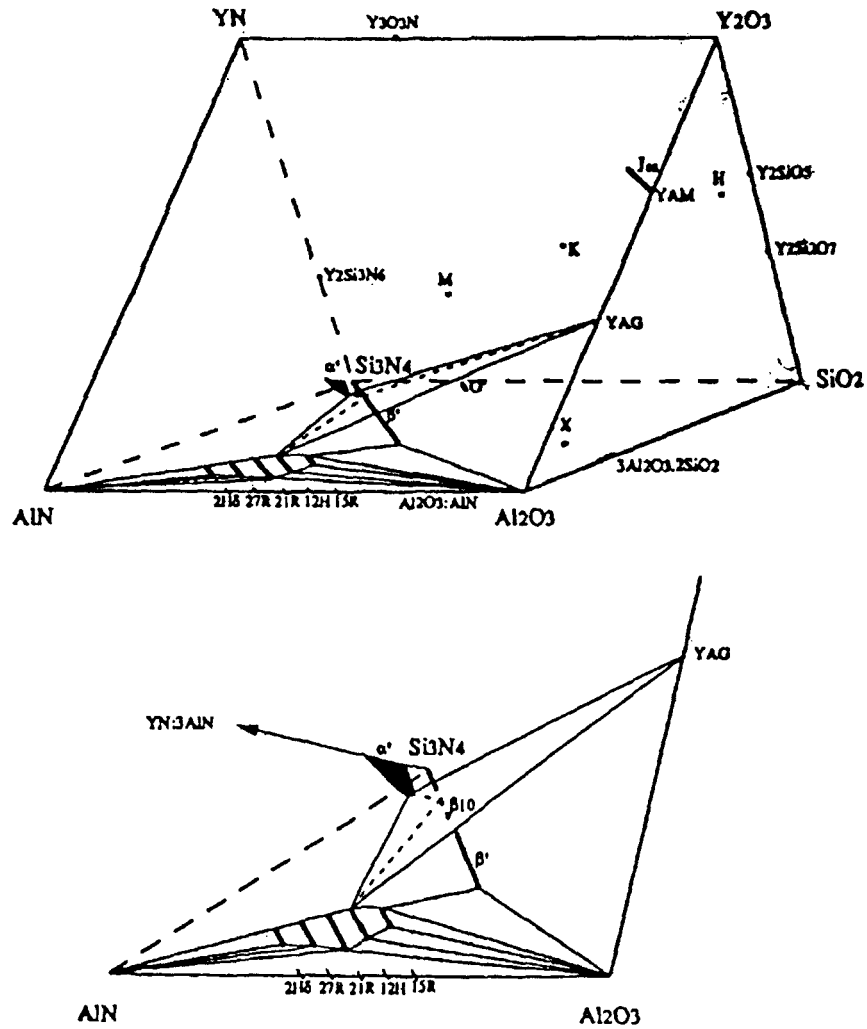


Fig. 5 Compatibility tetrahedron $\alpha'$-$\beta_{10}$-12H-YAG

treatment will devitrify the N-containing glassy phase to form refractory crystalline phase(s). It was thus, expected that the material will exhibit better high temperature properties. The compound additives we used were $Y_2O_3$ plus $La_2O_3$ and the subsolidus phase relationships in the system $Si_3N_4$-$Y_2O_3$-$La_2O_3$ have been determined. The comparison of the high temperature mechanical properties of these two types of $\beta Si_3N_4$ or $\beta$'-Sialon matrixed material is shown in Fig. 6. The specimens containing only 1 wt% $Al_2O_3$ start to show a drop in flexural strength above 1000°C, while those with only $Y_2O_3$ plus $La_2O_3$ retain their strength until 1300°C[16,17]. By further manipulating the additive contents with the aim to control the average grain boundary thickness at 4 or 8 nm, the strength retention capability of these materials has been shown to be enhanced to 1400°C or some what beyond (Fig. 7)[18,19]. Heat treatment under atmospheric condition at 1350°C leads to the crystallization of $LaYO_3$ along with the N-containing phases at the expense of a large part of the glassy phase at the grain boundaries. Their effect on materials strength from 1000-1400°C is

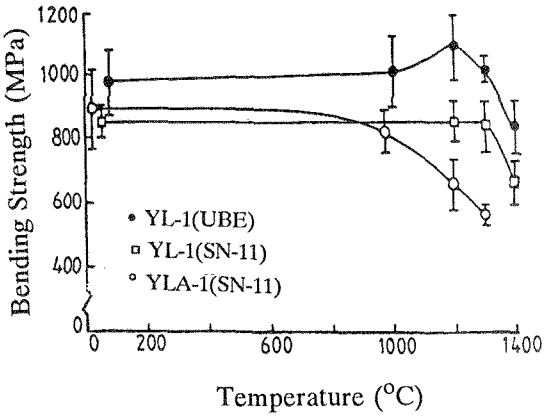


Fig. 6 Flexural strength vs temperature of YL-1 and YLA-1 materials

positive and may extend to even higher temperatures which will be a subject for further study. Moreover, the creep studies show that the materials with thinner grain boundary width (4 nm) and those that have gone through devitrification treatment exhibit noticeably lower creep strains at 1300°C under 250 MPa stress up to 200 hrs in comparison with those having 8 nm average grain boundary thickness (Fig. 8). Preliminary investigations indicate that the creep mechanism up to 1300°C is mixed with diffusional creep as the

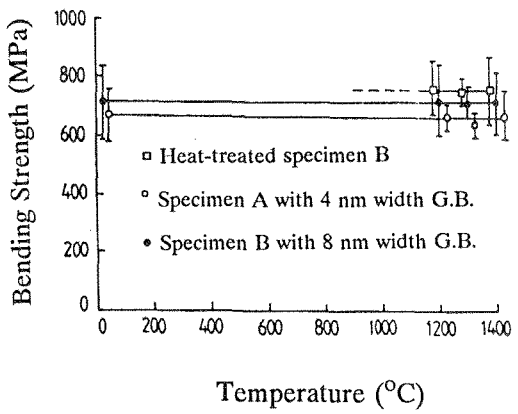


Fig. 7 Flexural strength vs temperature of specimens with 1:1 ratio of $Y_2O_3$:$La_2O_3$ additive content having controlled grain boundary width

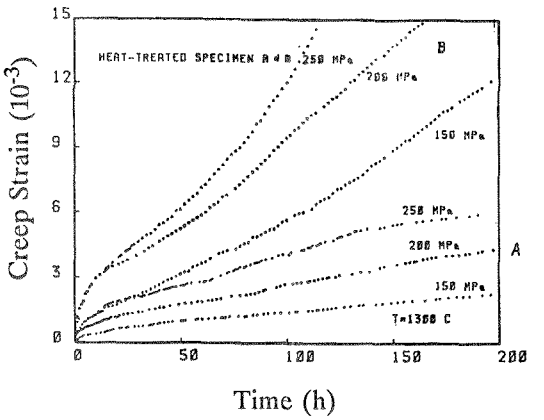


Fig. 8 Stress — Creep behavior of specimens with 4 and 8 nm average grain boundary thickness

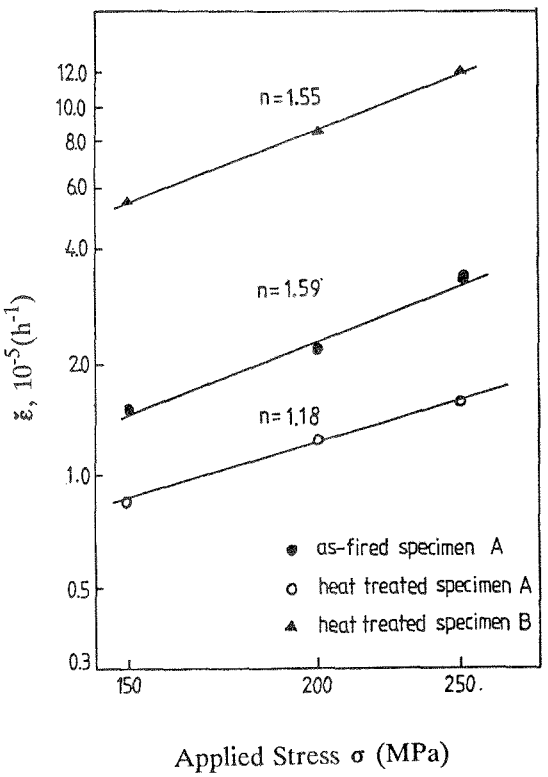


Fig. 9 The Log-Log Plot of Creep Rate vs Applied Stress for these Advanced Nitride Ceramics

controlling factor (Fig. 9). Cavitation can be seen at higher temperatures and higher stress.

## PROCESSING, MICROSTRUCTURE AND PROPERTIES OF ADVANCED CERAMICS

The properties of advanced ceramics with designed phase compositions are, to an appreciable extent, influenced by the microstructure developed through the choice and variations of processing routes. For this important area of materials research, the in-situ development of β'-Sialon in a matrix of equiaxed α'-Sialon phase will be discussed to illustrate the significant role of processing[20]. The composite Sialons were fabricated with α-$Si_3N_4$ (containing ~5% β-phase and 1.5 w/o O), AlN (1.5 w/o O) and $Al_2O_3$, $Y_2O_3$ (>99.9% pure) as starting powders to give a nominal weight ratio of α'-Sialon ($Y_{0.33}Si_{9.3}Al_{2.7}O_{1.7}N_{14.3}$) to β'-10 of 1 to 4 in the product. 2 wt% YAG was incorporated as the minimal amount of oxide additive to aid densification. The garnet was presynthesized and pulverized to insure homogeneous distribution of $Al_2O_3$ to $Y_2O_3$ in the mix. Full densification of the material with such little amount of additives was achieved by GPS at 1900°C, 1.5 MPa and a hold of 3h. Another measure was taken to manipulate the microstructure by influencing the nucleation and growth of the β'-Sialon phase by the addition of different amounts of fine β-$Si_3N_4$ seeds as additional nucleation sites. These β-$Si_3N_4$ powder was synthesized by SHS method having an average grain size of 0.3 μm. The amounts added were respectively 1, 2, 5, 8 and 12 wt%.

Through gas pressure sintering, the specimens were fully densified with a density of 3.27. They were then heat treated at 1350°C, 24h to devitrify the grain boundary glassy phase. XRD patterns show that the main crystalline phases are α'- and β'-Sialons with a weight ratio of 25 to 75 before heat treatment. After heat treatment, $Y_3Al_5O_{12}$ and some J-phase and K-phase are seen to recrystallize out from the glassy phase.

The microstructural change with β-$Si_3N_4$ seeding is very obvious (see Fig. 10). In the specimens with no seed, the β' - Sialon grains

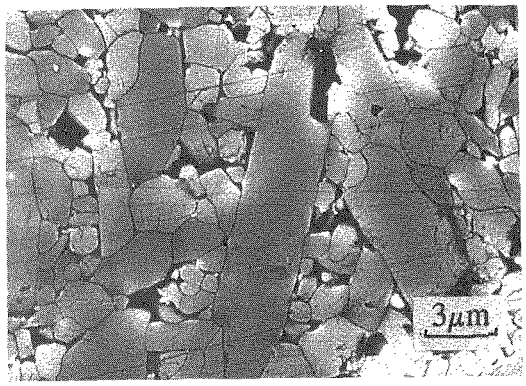


0% seed

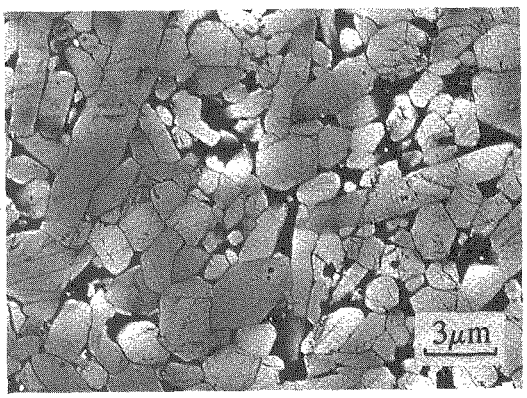


2% seed

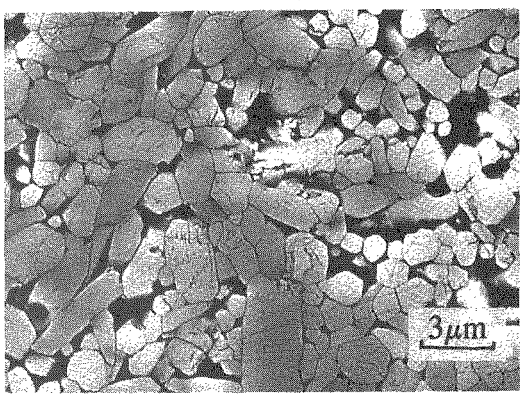


8% seed

Fig.10 The Microstructure of α'- and β'-Sialon Composite materials with 0, 2, and 8% β-$Si_3N_4$ Seed Addition

are fully developed into stout prisms with aspect ratios of 4-7. Those with 2% seed, the microstructure

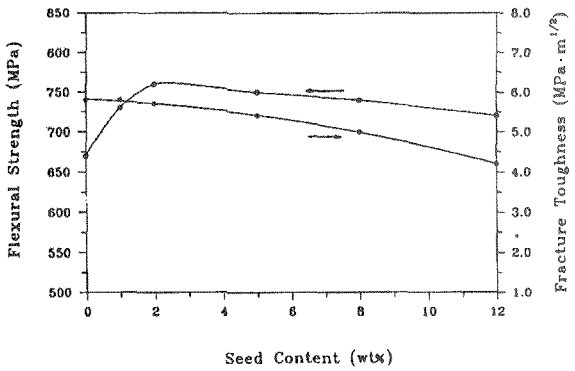


Fig.11 Some Mechanical Properties of α'- and β'-Sialon composite Materials with Different Contents of β-$Si_3N_4$ Seed Addition

of the β'-Sialon grains becomes much finer, maintaining large aspect ratios of 6-8. Further increase of seed addition to 8% gives a still finer microstructure with many more β'-grains of much smaller aspect ratios, around 2-4.

Fig.11 shows some of the mechanical properties of these Sialon composites with manipulated microstructural changes. The influence of microstructure on strength is more evident. The specimens with excessive growth of β'-Sialon grains (no seed addition) appear to have the lowest strength, due possibly to the development of large internal defects. Specimens with finer microstructure and large aspect ratio of β'-grains (2% seed) gives the highest strength. But

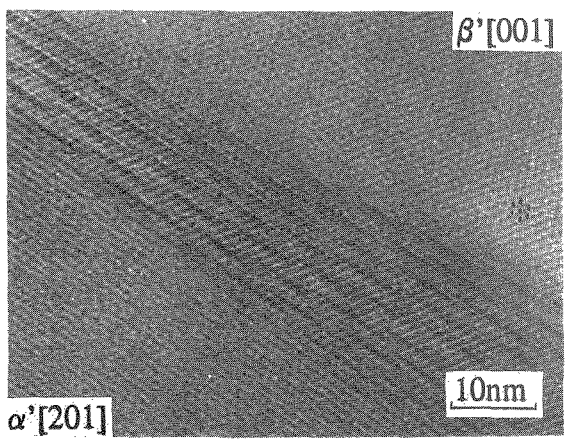


Fig.12 Coexistence of α'-Sialon with β'-Sialon through structural Modulation

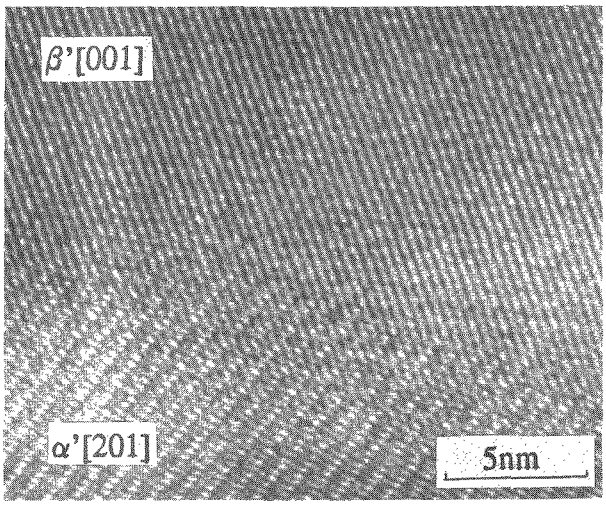


Fig.13 Coexistence of α'-Sialon with β'-Sialon through Lattice Mismatch

those with 5% and 8% seed, giving lower aspect ratio β'-grains do not seem to affect the strength to any appreciate extent. The fracture toughness values of those with 0, 1, and 2% seed addition appear to have not much difference. It would be interesting to investigate the R-Curves and the micromechanics around the crack tips of the specimens having this type of microstructure with high aspect ratio grains grown in-situ and to study the toughening mechanism in detail. Those specimens with 8% and 12% seed additions and having β'-Sialon grains of much lower aspect ratios do have somewhat lower fracture toughness values.

The high resolution electron microscopy study of these Sialon composites reveals some interesting features[21]. Since the oxide additive content is rather low and densification is achieved by gas pressure sintering, direct contact between α'-phase with β'-phase is commonly observed either through structural modulation (Fig.12) or through lattice mismatch (Fig.13). Post sintering devitrification at 1350°C results into almost complete crystallization of the intergranular glassy phase. Fig.14 shows the lattice image of a devitrified J phase. And a thin, disordered film of several nm thickness exists between the J phase and the preexisting α'-phase, labelled as G (Glassy phase). There have been some detailed discussion

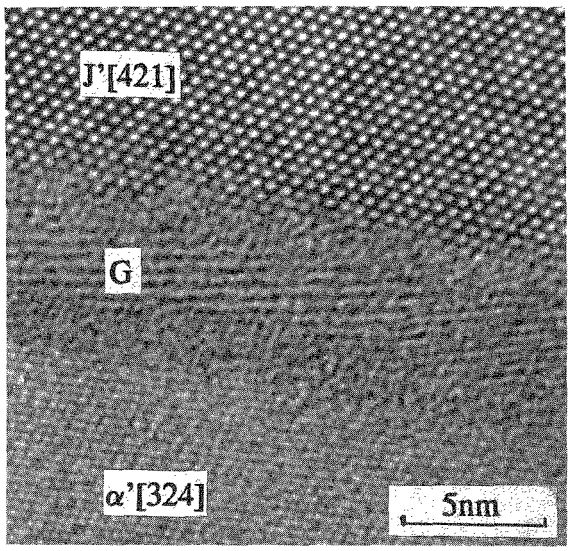


Fig.14 HREM showing the recrystallized J-phase and the Preexisting α'-Sialon Phase with a disordered thin film in between

on the existence of thin grain-boundary glassy films in silicon nitride ceramics[22]. Close examination of the G phase in between, there appears to have some orderliness in nanometer scale and is not completely random.

## STRENGTHENING AND TOUGHENING OF ADVANCED CERAMICS

Considerable work to strengthen and toughen mullite, TZP, and SiC materials have been carried out at several institutions in China. Mullite is a good material by showing little strength change from room temperature up to 1000°C and exhibit good thermal shock resistance. However, its strength and fracture toughness are comparatively low for more demanding performance requirements. Whisker or particulate reinforcement has been shown to be effective[23]. Zirconia toughened mullite in conjunction with particulate incorporation is even more effective to upgrade the strength of the composite material by more than two folds from ambient temperature up to 1200°C (Fig.15)[24]. Zirconia toughened mullite and whisker reinforced mullite both exhibit substantial enhancement in their toughness in

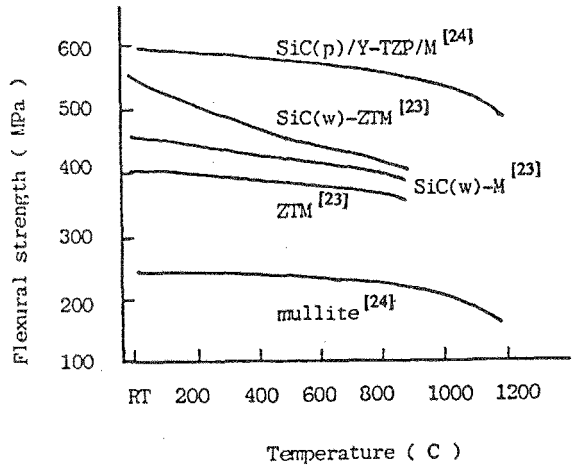


Fig.15 Dependence of Flexural Strength vs Temp. of Mullite based Composites

comparison with pure mullite material from room temperature to 800°C[23]. Again, particulate or whisker reinforcement in conjunction with transformation toughening on mullite give more impressive improvements in enhancing the fracture toughness of the mullite material[23,24]. These results are compiled in Fig.16. The mechanisms behind these phenomena are more or less clear. Apparently, crack deflection, debonding, and pull-out effect etc can have concurrent effect to

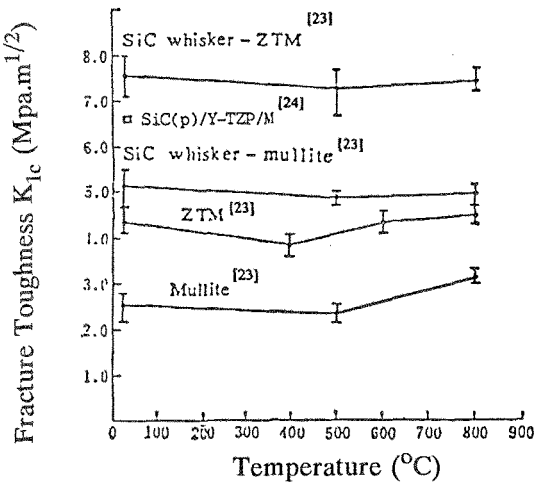


Fig.16 Dependence of Fracture Toughness vs Temp. of Multiphase Mullite Composites Ceramics

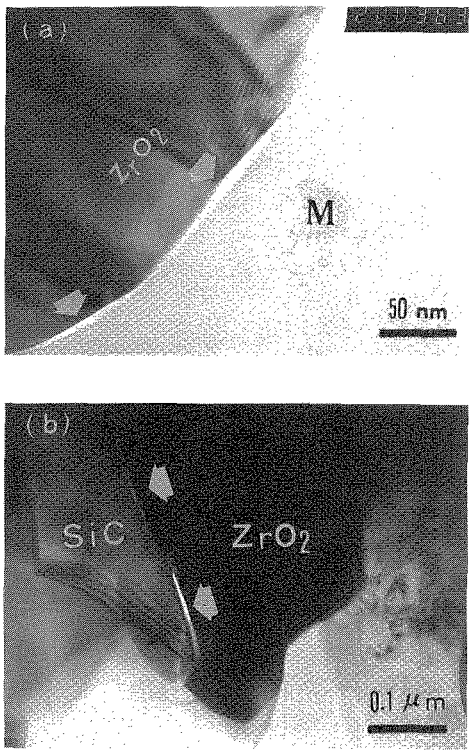


Fig.17 TEM Micrographs of $SiC_{(p)}$/Y-TZP/Mullite Composite Showing Microcracks at the $ZrO_2$-Mullite Interface (a), the SiC/$ZrO_2$ Interface (b)

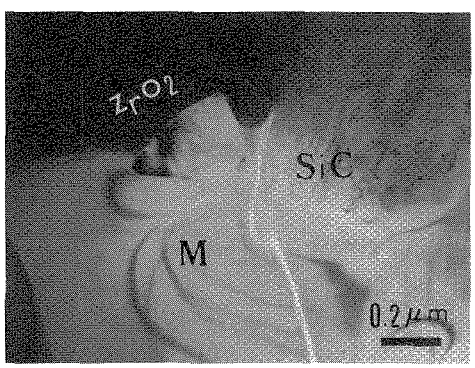


Fig.18 TEM Micrograph of $SiC_{(p)}$/Y-TZP/Mullite showing Crack Deflection by a SiC Particle

strengthen and toughen the materials studied, like mullite. However, the real situation can be much more complicated. Fig.17, 18 show microcracks

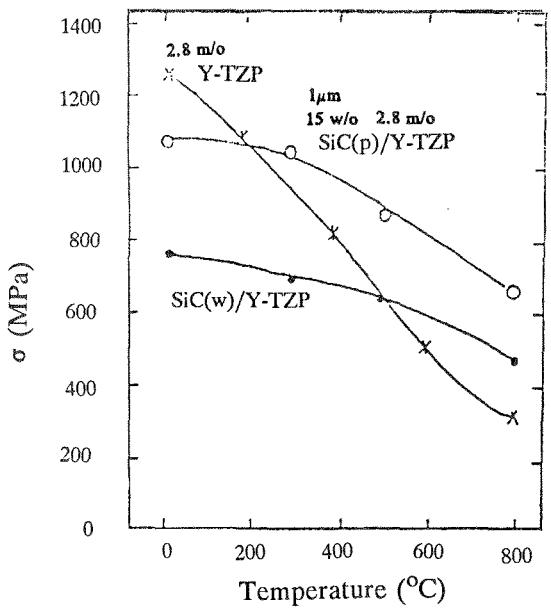


Fig.19 Strengthening of Y-TZP Composites at Higher Temperatures

developed between different phases and the crack deflection phenomenon. In-depth microstructural study of the composite material will be significant to be pursued.

Another material that has been studied is Y-TZP by incorporating $SiC_{(w)}$ or particulates to strengthen the material at higher temperatures. It is well known that Y-TZP material that is well processed can have very good room temperature strength and toughness. However, both the strength and toughness drop with temperature drastically[25,26]. Both SiC particulate and whisker incorporation showed evident strengthening effect at higher temperatures (Fig.19)[27,28]. Preliminary study indicates that the substantial drop of room temperature strength of $SiC_{(w)}$/Y-TZP composite in comparison with Y-TZP material is partially due to the uneven dispersion and distribution of the whisker in the matrix. Better processing can be of great help to achieve improvements. Fine SiC particulate incorporation (15 wt%, av. 1 μm particle size) gave more impressive strengthening effect. Its strength at 800°C is about doubled that of 2.8 Y-TZP material. Fig.20 shows a SiC particle situated intergranularly between TZP grains with glassy phase regions seen in between. However,

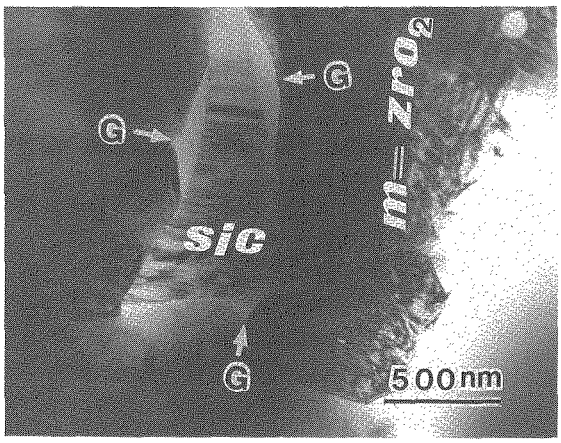


Fig.20 TEM Micrograph of $SiC_{(p)}$/Y-TZP Composite Showing Intergranular SiC Particle and the Glassy Phase (G), Some m-$ZrO_2$ Can Also Be Noted

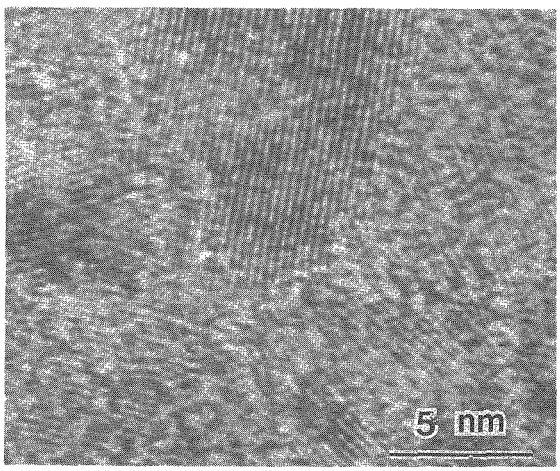


Fig.21 HREM Showing Lattice Images of Microcrystalline Structures in the Glassy Phase in $SiC_{(p)}$/Y-TZP Composite

high resolution study of the glassy phase revealed its microcrystalline fine structure in nanometer scale (Fig.21). Lattice images are clearly shown which indicated that of SiC. This phenomenon may help to explain the strengthening effect of the composite at higher temperatures with the presence of intergranular glass.

## BIOCERAMICS AND THEIR SUPERFINE MICROSTRUCTURE STUDIES

Bioceramics is becoming an increasingly important area of research in the materials community. It will be interesting to learn about the microstructures of natural bones or teeth comparing with those that are artificially fabricated. The essential constituent that forms the human bone and teeth is hydroxyapatite, an inorganic compound with its stoichiometric formula as $Ca_{10}(PO_4)_6(OH)_2$. The HR electron micrograph of which is shown in Fig.22. Comparing the microstructures of human teeth enamel and those artificially synthesized from chlorapatite, the differences are striking[29,30]. Fig.23 clearly shows that the human enamel is composed of crystals with much smaller sizes of about 30x30x200 nm in average which are preferentially aligned along the C-axis. While the synthetic hydroxy- or chlorohydroxyapatite material has a usual well sintered crystalline morphology. The grain sizes are larger with an average of 2-3 μm depending on the sintering temperature used[31] and there is no preferential alignment of crystalline orientations. And the high resolution electron micrographs of synthetic chlorapatite indicate clean grain boundaries where coherency between grains and very clean triple point can be seen. The situation of the grain boundaries of human dental enamel is entirely different. Foreign stuffs are always seen at

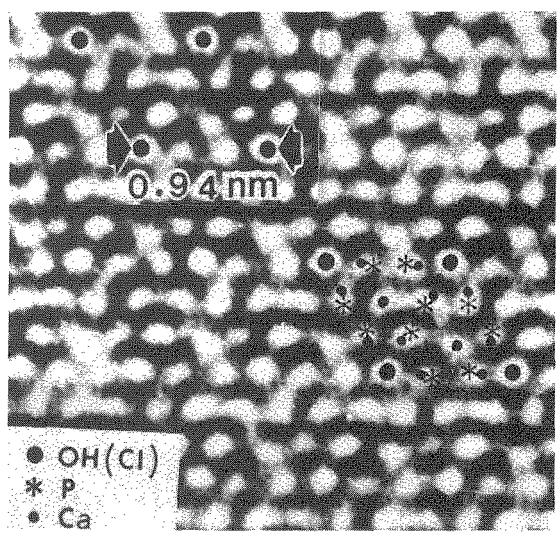


Fig.22 High Resolution and Atomic Arrangement of Hydroxyapatite Structure Viewed Along C Axis

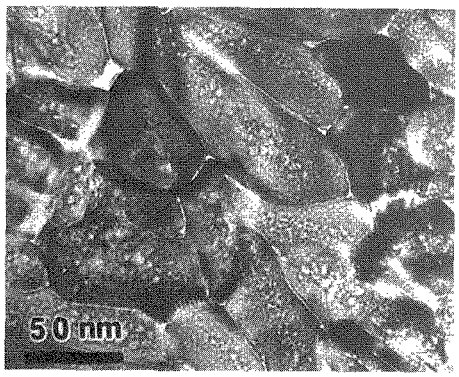


Fig.23 Microstructure of Human Tooth Enamel (essentially $Ca_{10}(PO_4)_6(OH)_2$)

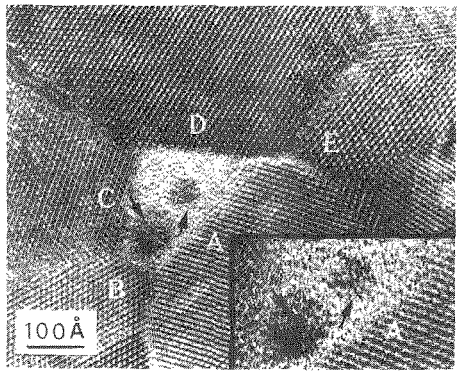


Fig.25 HREM of Human Tooth Enamel Showing Details of the Amorphous Region

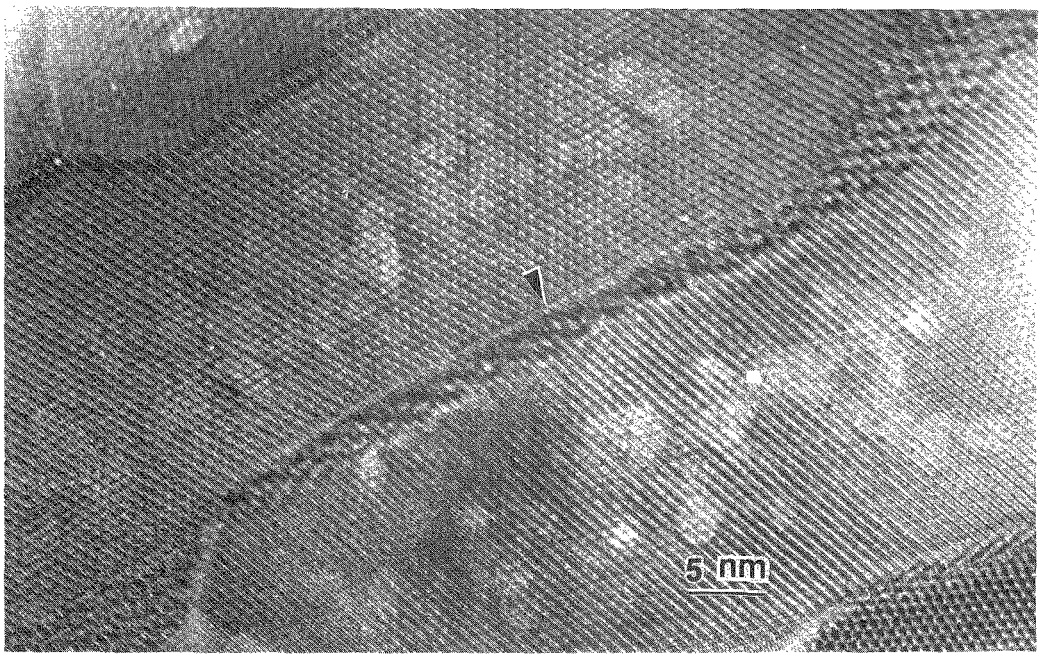


Fig.24 High Resolution Electron Micrographs of Human Tooth Enamel Showing Details of Grain Boundaries

the grain boundaries (see Fig.24). They are structurally and sometimes chemically different from that in the bulk of the grains. Fig.25 shows an amorphous region, surrounded by several grains, in which there seems to have a more orderly zone of 2-3 nm size. It has also been shown that these interfaces may include some inorganic ions, mainly $K^+$, $Na^+$, $Mg^{2+}$, $Cl^-$, $F^-$, in concentrations far greater than those of the neighboring apatite crystals. Clearly, bioceramics is a fascinating field of research. And biomimetic synthesis of materials is something that materials scientists can learn a lot from the nature.

## CONCLUDING REMARKS

It is the intention to discuss the importance of advanced inorganic materials by pinpointing a few frontier R&D areas and illustrated by some experimental results. The subject matters discussed are by no means exhaustive. However, it is more so the wish to invite discussions and comments and the author sincerely believe that the development of advanced ceramics will proceed at an even faster pace in the rest part of the nineties for the service of the advancement of human society.

## REFERENCES:


[1] W.Y. Sun, Z.K. Huang and J.X. Chen, Trans. Brit. Ceram. Soc., 82 (1983) 173

[2] Z.K. Huang, P. Greil and G. Petzow, J. Am. Ceram. Soc., 66 (1983) C96

[3] G.Z. Cao, Z.K. Huang, X.R. Fu and D.S. Yan (T.S. Yen), Intl. Jour. High Tech. Ceram., 1 (1985) 119

[4] W.Y. Sun, Z.K. Huang, G.Z. Cao and D.S. Yan, ibid, 3 (1987) 227

[5] Z.K. Huang, W.Y. Sun and D.S. Yan, J. Mater. Sci., Letters, 4 (1985) 255

[6] Z.K. Huang, T.Y. Tien and D.S. Yan, J. Am. Ceram. Soc., 69 (1986) C241

[7] S. Slasor, Ph.D. Thesis, Univ. of Newcastle upon Tyne, (1986)

[8] W.Y. Sun, D.S. Yan and T.Y. Tien, Ceram. Intl., 14 (1988) 199

[9] W.Y. Sun and T.S. Yen, Mater. Letters, 8 (1989) 145; ibid, 8 (1989) 150

[10] W.Y. Sun, L.T. ma, and D.S. Yan, Chin. Sci. Bull., 35 (1989) 1189

[11] Z.K. Huang, D.S. Yan and T.Y. Tien, J. Solid State Chem., 85 (1990) 51

[12] S.F. Kuang, Z.K. Huang, W.Y. Sun and T.S. Yen, J. Mater. Sci. Letters, 9 (1990) 69; ibid, 9 (1990) 72

[13] W.Y. Sun, T.Y. Tien and T.S. Yen, J. Am. Ceram. Soc., 74 (1991) 2547; ibid, 74 (1991) 2753

[14] W.Y. Sun, T.S. Yen and T.Y. Tien, Sci. in China, Series A, 35 (1992) 877

[15] C.Z. Cao, Z.K. Huang and D.S. Yan, "Phase Relationships in $Si_3N_4$-$Y_2O_3$-$La_2O_3$ System", Sci. in China (Series A), 32, 429-433 (1989)

[16] Y.R. Xu, L.P. Huang, X.R. Fu and T.S. Yen, Scientia Sinica, Series A, 28 (1985) 556

[17] Y.R. Xu, Ph.D. Thesis, the Shanghai Institute of Ceramics, (1988)

[18] T.S. Yen et al., Proceedings 7th CIMTEC, June 23-26, 1990, Montecatini, Italy, Ed. P. Vincenzini, pp701

[19] T.S. Yen, Centennial International Symposium, The Ceramic Society of Japan, Proceedings, Ceramics: Toward the 21st Century, Ed. N. Soga and A. Kato, (1991) 435

[20] Hao Hang, Ph.D. Thesis work, on-going (1993)

[21] Qian Liu, Ph.D. Thesis, on-going (1993)

[22] H.-J. Kleebe et al., MRS Sym. Proceedings, "Silicon Nitride Ceramics", Ed. I.-W. Chen, P.F. Becher, M. Mitomo, G. Petzow and T.-S. Yen, Vol 287 (1993) 65

[23] Z.F. Yang, H.Y. Xu, J.Q. Tan, Q. . Yuan and Y.R. Zhang, J. Chin. Ceram. Soc., 17 (1989) 467

[24] X.X. Huang, J.S. Hong and J.K.Guo, Proceedings of 4th Intl. Sym. on "Ceram. Mater. and Components for Engines", June 10-12, Göteborg, Sweden, (1991), Ed. R. Carlsson et al., (1992), 795

[25] B.S. Li, X.X. Huang, J.K. Guo and D.S. Yan, J. Inorg. Mater., 1 (1986) 129

[26] L. Gao, D.S. Yan and J.K. Guo, Scientia Sinica, Series A, (1988) 95

[27] X.X. Huang, J.K. Guo, L.H. Gui and B.S. Li, Proceedings 4th Inter. Symp. on "Ceram. Mater. and Components for Engines", Göteborg, Sweden, June 10-12 (1991), Ed. R. Carlsson et al., (1992) p757

[28] Y.F. Zhang, J.K. Guo, X.X. Huang and B.S. Li, J. Inorg. Mater., 6 (1991) 172

[29] S.L. Wen, J.W. Feng, T. Liand A. Liu, Proc. 11th Intl. Congr. on Electron Microscopy, Kyoto, Japan, (1986) 3071

[30] S.L. Wen, Electron Microsc. Rev., 2, (1989) 1

[31] A. Krajewski, A. Ravaglioli, S.L. Wen and J.W. Feng, J. Appl. Phys., 25 (1992) 465